The visual perception of metal

James T. Todd

Department of Psychology, The Ohio State University, Columbus, OH, USA

J. Farley Norman

Psychological Sciences, Western Kentucky University, Bowling Green, KY, USA

The present research was designed to examine how the presence or absence of ambient light influences the appearance of metal. The stimuli depicted three possible objects that were illuminated by three possible patterns of illumination. These were generated by a single point light source, two rectangular area lights, or projecting light onto a translucent white box that contained the object (and the camera) so that the object would be illuminated by ambient light in all directions. The materials were simulated using measured parameters of chrome with four different levels of roughness. Observers rated the metallic appearance and shininess of each depicted object using two sliders. The highest rated appearance of metal and shininess occurred for the surfaces with the lowest roughness in the ambient illumination condition, and these ratings dropped systematically as the roughness was increased. For the objects illuminated by point or area lights, the appearance of metal and shininess were significantly less than in the ambient conditions for the lowest roughness value, and significantly greater than in the ambient condition for intermediate values of roughness. We also included a control condition depicting objects with a shiny plastic reflectance function that had both diffuse and specular components. These objects were rated as highly shiny but they did not appear metallic. A theoretical hypothesis is proposed that the defining characteristic of metal (as opposed to black plastic) is the presence of specular sheen over most of the visible surface area.

Introduction

One of the great mysteries of human perception is the ability to tease apart how patterns of image shading are influenced by the shapes of objects, the pattern of illumination, and the manner in which light is structured by different types of materials (e.g., metal, glass, plastic, or wax). Some researchers have argued that the computation of any one of these factors from image data requires that the other two factors be known a priori, perhaps through the use of statistical priors (e.g., Wijntjes, Doerschner, Kucukoglu, & Pont, 2012). However, our anecdotal experience in the natural environment suggests that we are able to simultaneously identify these factors—at least to a first approximation.

The perception of three-dimensional (3D) shape from shading has been an ongoing area of research since the 1980s (e.g., Mingolla & Todd, 1986; Todd & Mingolla, 1983), but the study of perceived illumination and material properties has primarily occurred during the past decade. Much of this research has focused on the perception of gloss. This research has examined the statistical properties of images depicting matte or shiny materials (Motoyoshi & Matoba, 2012; Motoyoshi, Nishida, Sharon, & Adelson, 2007). It has documented how apparent glossiness depends on the alignment of highlights and lowlights with surface curvature and diffuse shading (Anderson & Kim, 2009; Beck & Prazdny, 1981; Kim, Marlow, & Anderson, 2011, 2012; Marlow, Kim, & Anderson, 2011, 2012; Todd, Norman, & Mingolla, 2004) and how it can be affected by the pattern of illumination or the density of bumps in the surface geometry (Doerschner, Boyaci, & Maloney, 2010; Fleming, Dror, & Adelson, 2003; Ho, Landy, & Maloney, 2008; Marlow & Anderson, 2012, 2013; Mooney & Anderson, 2014; Nishida & Shinya, 1998; Olkkonen & Brainard, 2010, 2011; Pont & te Pas, 2006; Wijntjes & Pont, 2010). It has also shown how the perception of gloss can be influenced by other sources of information about 3D shape such as motion or stereo (Doerschner et al., 2011; Marlow & Anderson, 2015).

One important issue that has received relatively little attention in the literature is the ability of observers to distinguish among different types of shiny materials such as metal, porcelain, or glass (Fleming, Wiebel, & Gegenfurtner, 2013; Sharan, Rosenholtz, & Adelson, 2014; Vangorp, Barla, & Fleming, 2017). For example, consider the two objects presented in Figure 1. The one on the left has purely specular reflections and is

Citation: Todd, J. T., & Norman, J. F. (2018). The visual perception of metal. *Journal of Vision*, *18*(3):9, 1–17, https://doi.org/10.1167/18.3.9.

https://doi.org/10.1167/18.3.9 Received September 6, 2017; published March 23, 2018 ISSN 1534-7362

Figure 1. Images of a smoothly curved object with a metal (left) and shiny plastic (right) reflectance function.

immediately identified as metal by naïve observers. The one on the right, in contrast, has a linear combination of diffuse and specular reflections and is typically identified as shiny white plastic or porcelain. To better understand diffuse and specular reflections, it is useful to consider a small local surface patch that is visible to an observer. If that patch has a diffuse (Lambertian) reflectance function, then all incident light will be scattered equally in all directions, and any incident light beam from any possible direction will reflect a small portion of its energy toward the point of observation. Thus, the luminance gradients produced by Lambertian reflections tend to be relatively small. If, on the other hand, a visible surface patch has little or no roughness (as in shiny metals), then there is only a tiny range of incident directions for which any light will be reflected toward the point of observation. Because the light reflected from those incident directions is only minimally scattered, the energy that reaches the point of observation can be quite intense. This results in much higher luminance gradients than for Lambertian surfaces, with bright specular highlights and also dark regions where incident directions of illumination are outside the small range that reflect toward the point of observation.

It is a well-known problem in photography that shiny metal materials can be difficult to photograph because of the glare produced by specular reflections. Studio photographers avoid this problem by carefully controlling the pattern of illumination, so that a surface receives light from many different directions without introducing intense highlights from luminous sources (Hunter, Biver, & Fuqua, 2007). One technique for achieving this is called *soft box* or *white box* photography, in which an object is photographed inside a white box or tent. The sides of the walls are typically translucent to allow soft light to enter from the outside, and the surface interreflections inside the box provide a richly structured pattern of ambient light. Both of the images in Figure 1 were created using a simulation of that method, and a similar technique has been used previously for psychophysical research by Zhang, de Ridder, and Pont (2015).

Many simulations of shaded objects used in psychophysical experiments have illuminated scenes using isolated point or area lights without any ambient light at all. This is probably the optimal pattern of illumination for the depiction of matte surfaces because it maximizes image contrast. However, if a shiny metal object is rendered or photographed with that type of illumination the resulting image will be entirely black, except for some isolated highlights whose density will vary with the number of bumps on a surface (Ho et al., 2008; Marlow & Anderson, 2013). These observations suggest that the appearance of polished metal may be critically dependent on the pattern of ambient light in a scene.

The research described in the present article was designed to investigate the metallic appearance and shininess of objects in a variety of contexts. The goals of this research were threefold: first, to investigate the abilities of observers to distinguish between metal and shiny plastic materials; second, to assess how the perception of these materials is affected by the presence or absence of ambient light in a scene; and, finally, to investigate potential interactions between the pattern of illumination and surface roughness on judgments of metallic appearance and shininess.

Methods

Stimuli

The stimuli employed in the present study were created using Maxwell Render software developed by

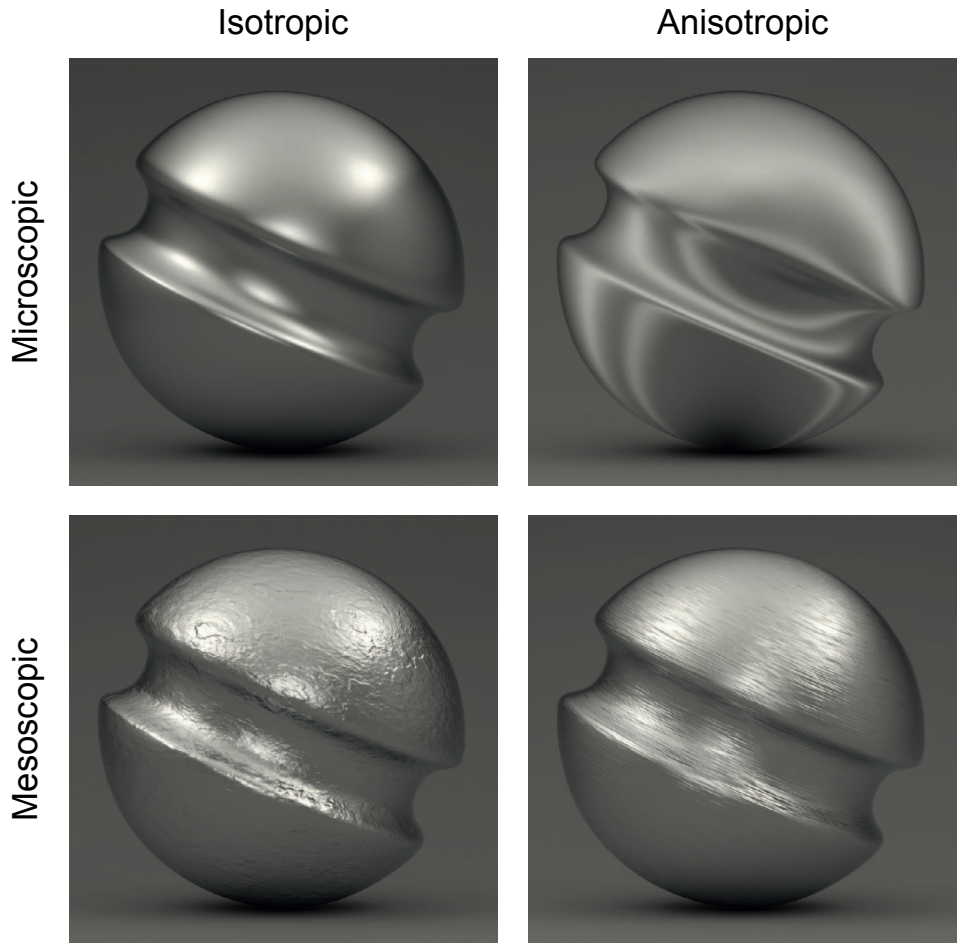

Figure 2. Objects with isotropic and anisotropic textures at microscopic and mesoscopic scales.

Next Limit (Next Limit Technologies, Madrid, Spain). It uses a variety of parameters to simulate how surfaces reflect light. The first of these is roughness, which controls the degree of microscopic scattering on a surface. A surface with roughness zero is perfectly smooth, whereas one with roughness 100 scatters light uniformly in all directions. Anisotropy and direction parameters control the directionality of the specular reflections. Anisotropic reflections occur on surfaces with microgrooves that run in one dominant direction, so that light reflects in a specular way in the direction of the grooves, and in a more diffuse way in the direction perpendicular to the grooves. The effects of this parameter are greatest for low values of roughness, and diminish to zero as the roughness approaches 100 (i.e., Lambertian reflectance). Microscopic anisotropic reflections are most commonly observed on cloth materials, such as satin, composed of tightly woven, smooth threads. It is important to recognize that the roughness parameter is designed to simulate surface texture at a microscopic scale that is not visible to the naked eye. It is also possible to create surface texture at larger mesoscopic or macroscopic scales by applying a bump or displacement map onto a surface, and these textures can also have varying degrees of anisotropy. Figure 2 shows images of a single object with the four different types of texture described above. All of the depicted objects have a microscopic texture with a roughness of 15, and the ones in the bottom row also have mesoscopic textures. The textures in the left column are isotropic, whereas the ones in the right column are anisotropic. In all of the discussion hereafter, the term roughness will be used to describe isotropic textures at a microscopic scale.

Two other parameters of the Maxwell renderer involve the index of refraction (IOR) of a material. The IOR is a complex number. The real part (n) is based on the speed of light in a material, whereas the imaginary part (k) is based on the propensity of a material to absorb light. This imaginary component is also referred to as the extinction index or the coefficient of extinction. The website https://refractiveindex.info provides a convenient resource to obtain the measured values of n and k for a wide variety of natural and man-made materials. For nonmetallic materials, the value of k is almost always close to zero, but that is not the case for metals. Using the Fresnel equations and the IOR for any given material, it is possible to compute the

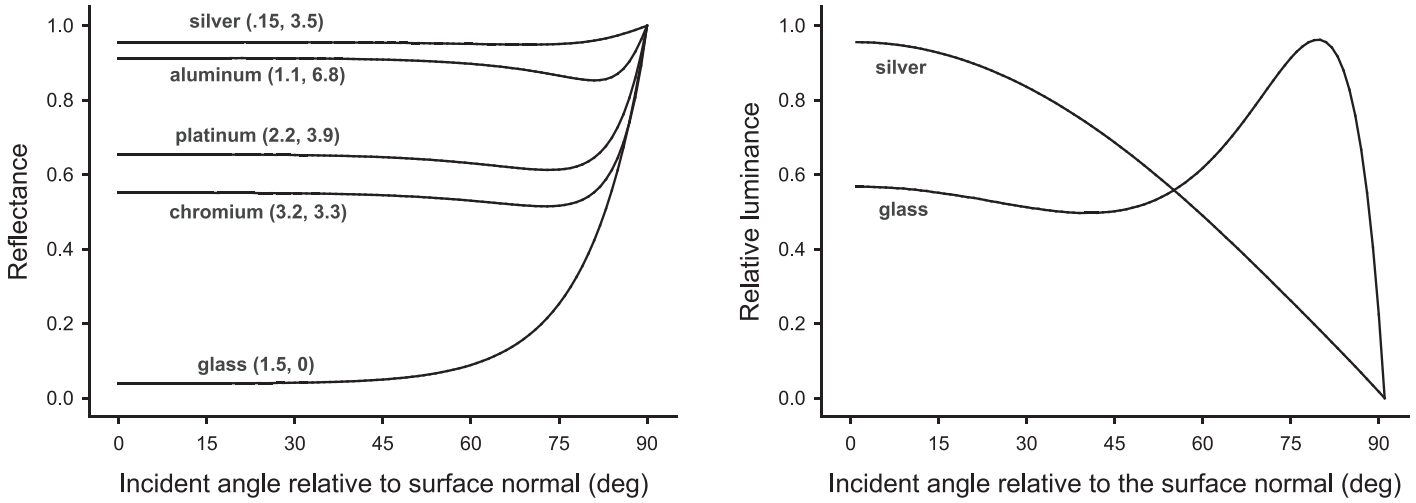

Figure 3. The left panel shows reflectance as a function of the incident angle for five common materials in unpolarized light. The numbers in parentheses show the index of refraction (*n, k*). The right panel shows the relative luminance of glass and silver as a function of the incident angle. These curves have been normalized to compensate for the large difference in the magnitude of specular reflections for these materials.

percentage of incident light that is reflected (i.e., reflectance) as a function of the incidence angle relative to the surface normal. The left panel of Figure 3 shows the functions for five natural materials, which were obtained using the Fresnel calculator at the website, http://unicorn.ps.uci.edu/calculations/fresnel/twophase.html. Note in particular how the effect of incident angle (i.e., the Fresnel effect) varies dramatically among different materials. For silver, almost all illumination is reflected at all incidence angles. For glass, on the other hand, very little light is reflected except at high incidence angles. Another thing to note about the Maxwell reflectance model is that roughness and IOR interact with one another. The effects of IOR are greatest for low values of roughness, and diminish to zero as the roughness approaches 100 (i.e., Lambertian reflectance).

It is important to keep in mind that the light reflected toward the point of observation (i.e., luminance) is a product of reflectance and illumination, and that illumination varies as a cosine function of the incidence angle, which is the geometric basis for Lambert's law. Thus, it is possible to compute the luminance of specular reflections by multiplying the reflectance values derived from the Fresnel equations times the cosine of the incident angle. The right panel of Figure 3 shows the relative luminance as a function of the incident angle for both glass and silver. These curves have been normalized to compensate for the large difference in the magnitude of specular reflections for these materials. Note that the luminance varies as a cosine function of the incident angle for silver, but that the effect of incident angle is more complex for glass. The maximum luminance in that case occurs at an incident angle of 79°. Figure 4 shows two spherical objects illuminated by a high dynamic range image (HDRI) of a banquet hall. The material depicted in the left panel is purely specular with an IOR of silver, whereas the one on the right is purely specular with an IOR of glass. Because silver reflects a much higher proportion of the incident light than glass, the exposure of the glass image has been increased appropriately so that both images have the same maximum luminance. Despite that normalization, however, the two images appear quite different. Note that the glass reflections are much dimmer in the interior portions of the sphere and brighter in the periphery due to the Fresnel effect. This is the pattern of specular reflection that is typically observed on nonmetallic shiny objects in the natural environment.

It is also possible in the Maxwell renderer to combine different materials to create a linear combination of reflectance properties. Two component reflections are common in many man-made materials. For example, paints are typically emulsions of two types of molecules called pigments and binders. The pigments tend to scatter and absorb light, whereas the binders are transparent and produce specular reflections. The glossiness of paint is determined by the relative proportion of pigment and binder. Glossy paints have a high proportion of binder. The pigment molecules in that case mostly lie below the surface of the emulsion creating a smooth layer of binder molecules that produce specular reflections. Matte paints, in contrast, have a high proportion of pigment molecules, which can protrude above the surface boundary and limit the amount of specular reflections.

It is interesting to contrast the Maxwell reflectance model with one proposed by Ward (1994) that has been used in many previous psychophysical experiments.

Figure 4. Images of a spherical object with purely specular reflections. The material depicted on the left has an index of refraction (IOR) of silver, which produces a negligible Fresnel effect (i.e., the same percentage of light is reflected at all incidence angles). The image on the right has the same IOR as glass, which produces a much larger Fresnel effect. This is the typical pattern of reflection for most nonmetal shiny materials in the natural environment. The exposures of these images have been adjusted so that they have the same maximum luminance.

The Ward model treats surface reflections as a weighted combination of two components: a diffuse (Lambertian) component, in which some proportion of the incident light is scattered uniformly in all directions; and a specular component, in which scattering is limited to a smaller range of directions. The extent of specular scattering is controlled by a roughness parameter. An important limitation of this model is that it does not simulate the Fresnel effect for reflections. It is in effect a linear combination of a purely Lambertian material and one with the reflectance properties of silver. However, most of the lacquers and binders used in the real world have optical properties that are quite similar to glass as opposed to silver. There is other rendering software available, such as V-Ray, Blender, or finalRender, that are able to simulate the Fresnel effect, but only for nonmetal materials for which the value of k is zero. We are unaware of any psychophysical studies that have exploited these capabilities to study the perceptual analysis of image shading.

Another complication of real world materials is that the values of n and k vary as a function of wavelength. The Maxwell renderer includes a library of materials with measured IORs at many different wavelengths. The use of these materials enhances the photorealism of a scene, but with a cost of increased rendering time. The simulations of metal objects in the present study used the measured chrome material from this library. We also used a shiny white plastic material in which Lambertian reflection was combined with the specular properties of glass. This was included as a control to show that perceptually shiny materials need not appear metallic.

The stimuli for this experiment were generated using three different patterns of illumination, which are shown in Figure 5 as reflected in a perfectly smooth mirrored sphere. These included a translucent white

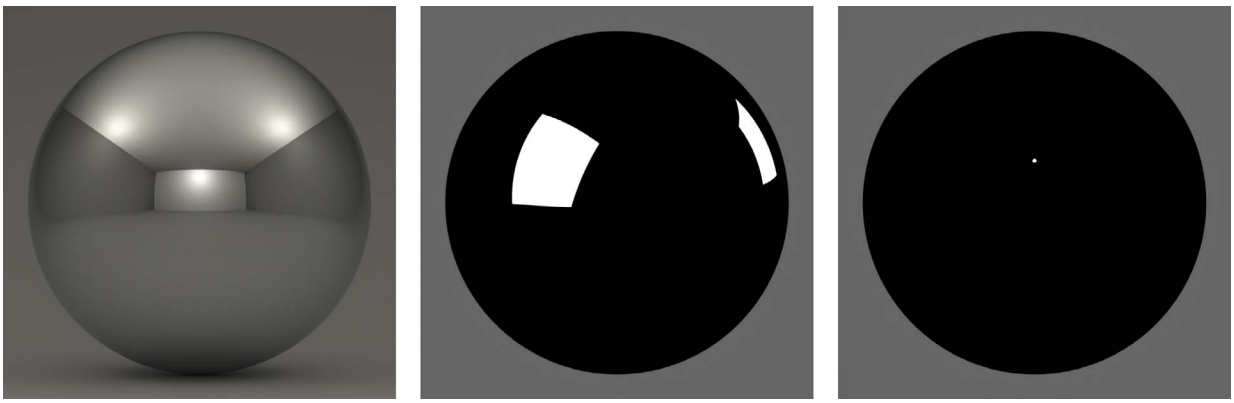

Figure 5. The three illumination fields used in the present experiment as reflected from a perfectly smooth mirrored sphere.

room identical to the one used for the images in Figure 1; a pair of rectangular area lights, one to the left in front of the object and another to the right behind the object; and a small spherical light directly in front and above the object. These were intended to span the range between illumination from all directions (i.e., the white room) to illumination from a single direction (i.e., the point light), and the area lights were included as an intermediate case.

The stimuli depicted three different objects: a sinusoidally deformed sphere (see Norman & Todd, 1996; Todd & Norman, 1995), a rounded circular disk with an embossed pattern of circular ridges, and a spherical object covered with small bumps. This last object was kindly provided by Scott Mooney and has been used in a previous study by Mooney and Anderson (2014). These particular objects were chosen to provide some variation in the overall patterns of curvature. The embossed disk is the most heterogeneous in this regard. It combines large areas that are completely flat with localized areas of very high curvature at the bases and tips of the circular ridges. The bumpy sphere, in contrast, has relatively large curvedness almost everywhere, and the deformed sphere has relatively low curvedness almost everywhere (see Koenderink, 1990). The objects depicted with chrome materials had four possible levels of microscopic roughness (15, 30, 60, and 97). All of the different chrome stimuli are shown in Figures 6 through 8. Each of these figures shows a single object with all possible combinations of illumination and roughness.

Figure 9 shows the shiny plastic stimuli for each combination of illumination and object. The intensities of the light sources and/or the camera exposure were adjusted for each stimulus so that the maximum image intensity would fall just below the maximum possible intensity of the display monitor.

Apparatus

The experimental stimulus images were displayed by an Apple Mac Pro computer (Dual Quad-Core processors, with ATI Radeon HD 5770 hardware-accelerated graphics) using an Apple 27-inch LED Cinema Display (2,560 × 1,440 pixel resolution). The monitor was located at a 100 cm viewing distance.

Procedure

For each of the 45 stimulus images, the observers estimated the metallic appearance and shininess of the depicted surface (i.e., bumpy spheres, sinusoidally modulated spheres, embossed disks). The observers rated these qualities by adjusting a slider (shown below the rendered surfaces) with the computer mouse. For judgments of metallic appearance, one end of the slider was labeled "does not look metallic at all," while the opposite end was labeled "could not look more metallic"; the midpoint of the slider was labelled "looks somewhat metallic." For shininess judgments, one end of the slider was labeled "not at all shiny," while the opposite end was labeled "maximally shiny"; the midpoint of the slider was labelled "moderately shiny." The possible rating magnitudes ranged from zero at one end of the slider (e.g., not at all shiny or metallic) to 100 at the opposite end (e.g., maximally shiny or metallic). While the observers usually made their judgments quickly (within several seconds), the observers could take as long as they wished to evaluate the depicted surfaces. At the beginning of each session, observers were shown the experimental setup, instructed about the rating scale, and allowed to perform a few trials of practice. During their debriefings, they all reported that they felt comfortable with the task, and had a high degree of confidence in their ratings for most of the stimulus images.

Observers

There were a total of seven observers (mean age was 23.7 years, range was 20 to 39 years). All observers possessed normal or corrected-to-normal visual acuity, and they were completely naïve about the purpose of the experiment or how the stimuli were created. Each of the observers judged all of the possible stimuli in a single experimental session.

Results

An analysis of variance on the observers' judgments of metallic appearance revealed a significant effect of material properties, $F(4, 24) = 49.28$, $p < 0.001$ and a significant interaction between materials and the pattern of illumination, $F(8, 48) = 17.84$, $p < 0.001$. None of the other comparisons in the analysis were statistically significant. The same pattern of results was also obtained for the ratings of shininess. There was a significant effect of material properties $F(4, 24) = 16.1$, $p < 0.001$, and a significant interaction between materials and the pattern of illumination, $F(8, 48) = 7.68$, $p < 0.001$, but none of the other comparisons were significant.

Figure 10 shows a comparison between the lowest roughness metal material (i.e., the top rows of Figures 6 through 8) and the shiny plastic material (i.e., Figure 9) for judgments of metallic appearance and shininess for

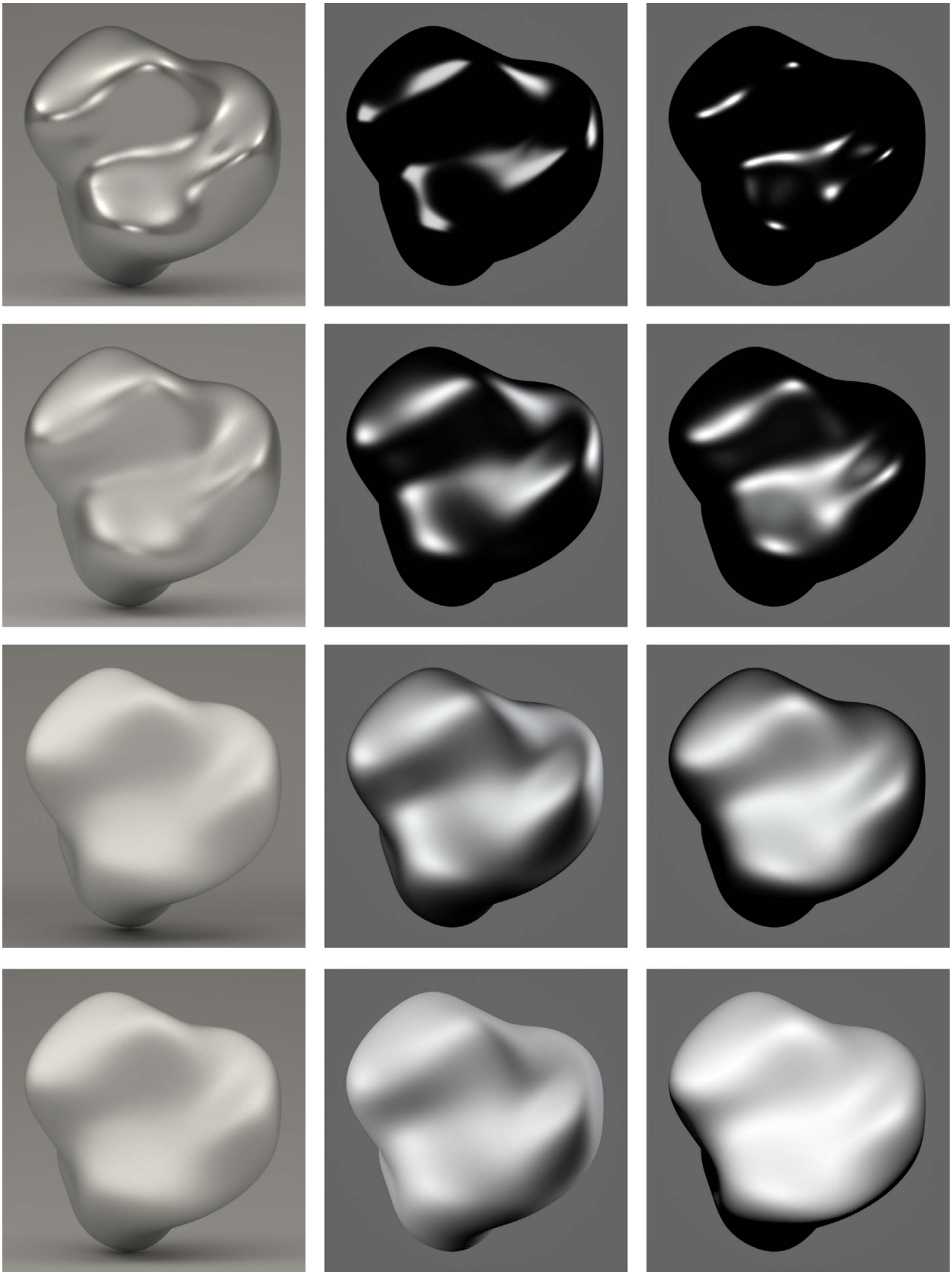

Figure 6. Images of a deformed chrome sphere with different lighting and roughness. The columns from left to right show the ambient, area, and point light illumination. The rows from top to bottom show roughness values of 15, 30, 60, and 97.

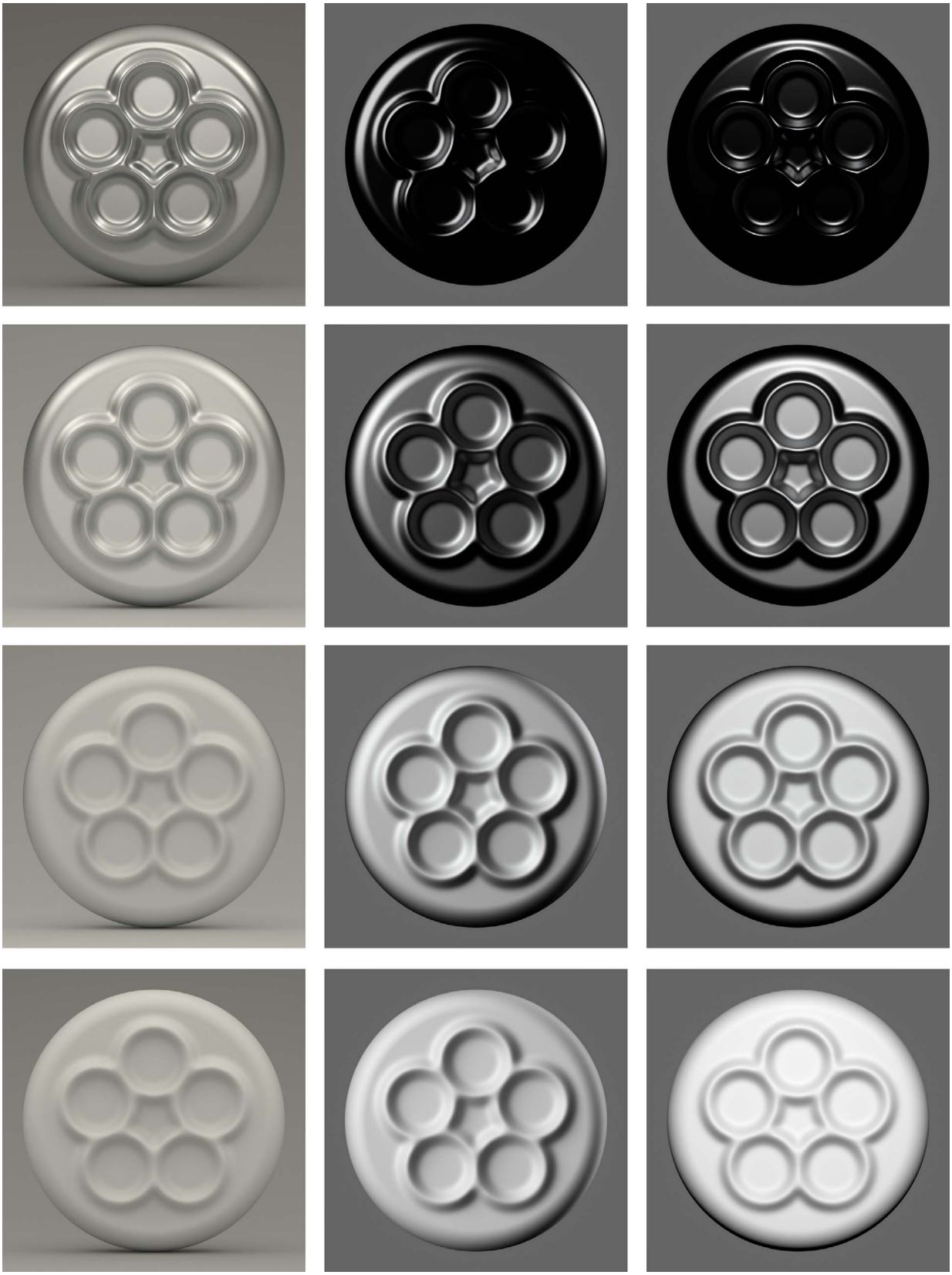

Figure 7. Images of an embossed chrome disk with different lighting and roughness. The columns from left to right show the ambient, area, and point light illumination. The rows from top to bottom show roughness values of 15, 30, 60, and 97.

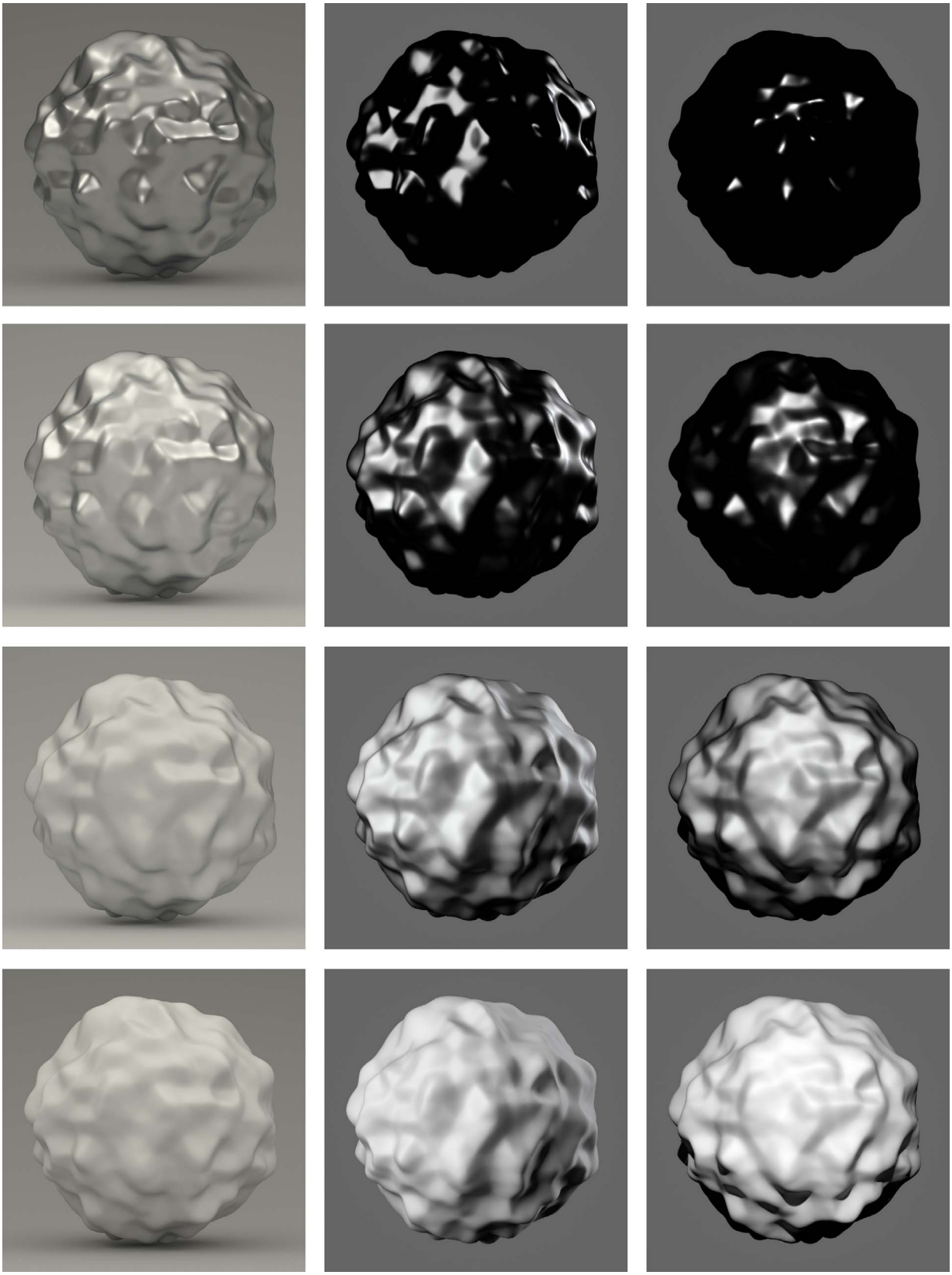

Figure 8. Images of a bumpy chrome sphere with different lighting and roughness. The columns from left to right show the ambient, area, and point light illumination. The rows from top to bottom show roughness values of 15, 30, 60, and 97.

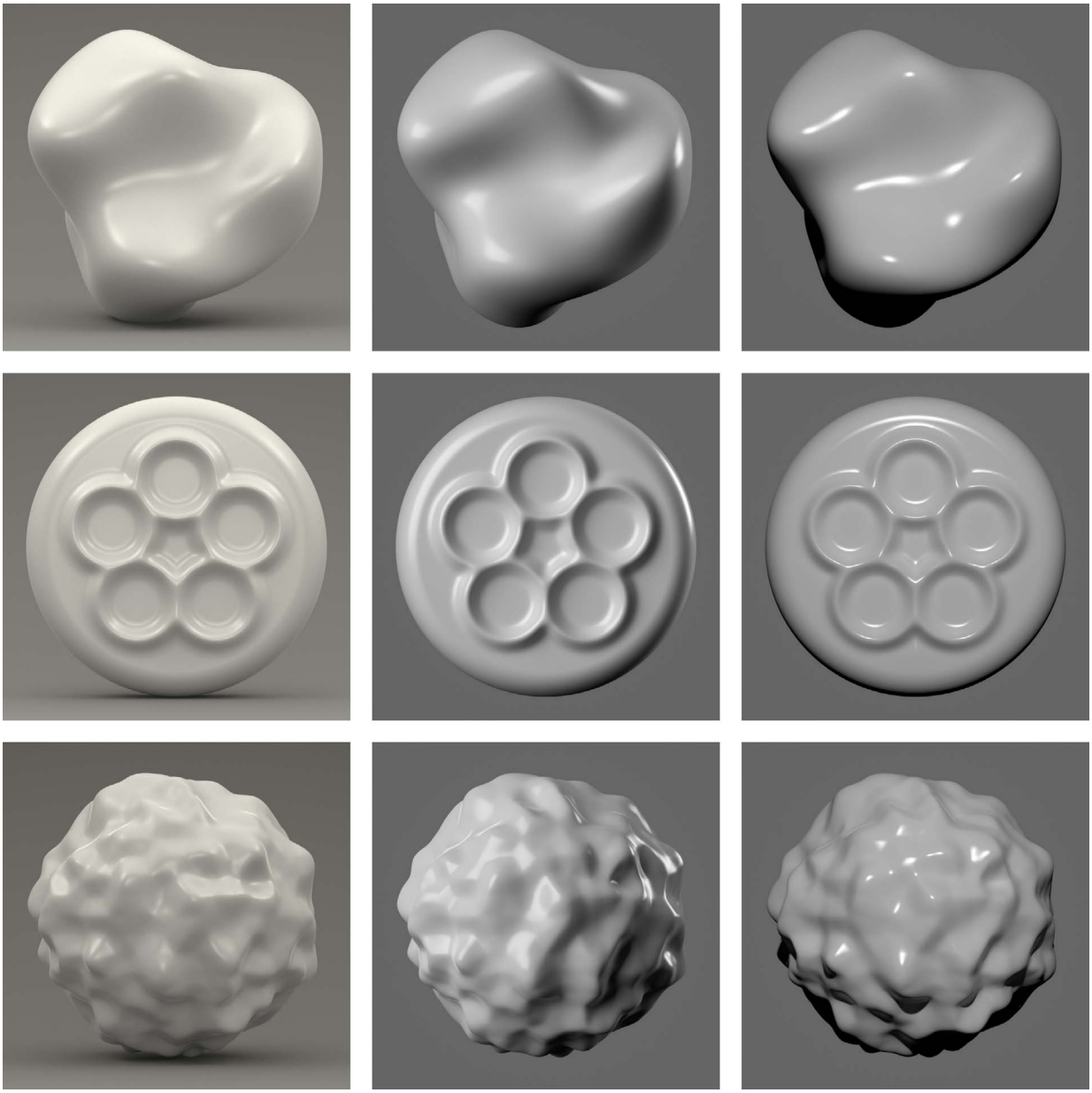

Figure 9. Images of shiny plastic objects with different lighting. The columns from left to right show the ambient, area, and point light illumination. The rows from top to bottom show the deformed sphere, the embossed disk, and the bumpy sphere.

each of the three objects. The highest metallic ratings were obtained for the chrome material with an ambient illumination. The average rating for those displays was 90 on a scale where 100 indicates that surface "could not look more metallic." The low roughness chrome with point or area illumination produced an average rating of only 37, and the judged metallic appearance of the plastic material was even lower with an average rating of 15. The highest shininess ratings were also obtained for the chrome material with ambient illumination. The average rating for those displays was 85, whereas the plastic materials and low roughness chrome with point or area illumination produced an average rating of only 59. Based on the earlier work of Marlow and Anderson (2013), it might be reasonable to expect that the shininess ratings for the plastic materials might have been higher if we had used a darker Lambertian component to increase the specular contrast of the displays. However, it should also be noted in this regard that the low-roughness metal objects illuminated by point or area lights had the highest possible specular contrast, yet the judged shininess for those displays was not significantly different from those obtained for the white plastic objects.

Over the course of this investigation, we have shown subsets of the stimuli to numerous observers in informal settings, and have asked them to describe the

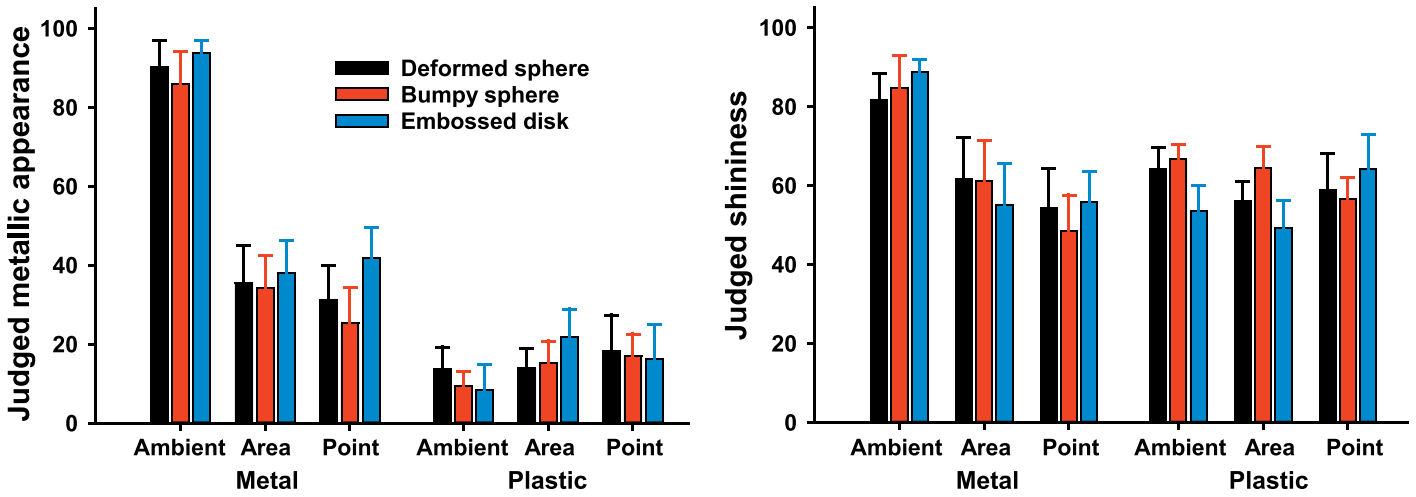

Figure 10. The average judged metallic appearance (left) and shininess (right) for low-roughness metal and shiny plastic for the three possible patterns of illumination. Error bars show the standard error of the mean for each condition.

depicted materials. When observers are presented with the white plastic objects in any of the three illumination fields, they invariably report that the objects appear as a shiny white material, such as plastic or porcelain. For low-roughness metal objects illuminated in the white room, they invariably describe the objects as metallic. Observers' descriptions are more variable when presented with images of low-roughness metal objects illuminated by point or area lights. They sometimes report that the objects appear vaguely metallic, or that they cannot be identified. However, the most common description for those displays is that the objects appear as a shiny black material, such as plastic or onyx.

Figure 11 shows the effect of roughness on judgments of metallic appearance and shininess for the chrome materials. For objects depicted in a translucent white room, the metallic appearance and shininess dropped rapidly with increasing roughness, and both were effectively eliminated for roughness values of 60 or above. However, for objects illuminated by point or area lights, the effects of roughness were nonmonotonic. As roughness was increased from 15 to 30, metallic appearance and shininess increased as well, but then dropped gradually toward zero as roughness was increased still further to 60 or 97. This effect was especially pronounced for the judgments of metallic appearance.

Discussion

One important difference between metal and plastic materials is that the specular reflections of metals are much more intense than those that occur on plastic materials (see Figure 3). This was not a relevant factor for observers' judgments in the present experiment, because the maximum image intensity was equated for all of the different stimuli. Despite that normalization, there were still clear differences in the categorical appearance of these stimuli. It should not be surprising that the shiny white plastic objects appeared shiny and nonmetallic. A more interesting result, however, is that the low roughness metal materials could appear as either metal or shiny black plastic depending on the pattern of illumination.

What are the image properties on which these perceptual distinctions are based? One possible hint to address this question comes from observers' subjective reports. When describing the appearance of shiny metal surfaces, they often use the term *metallic sheen*. In order to unpack what might be meant by that it is useful to review some previous research on the perception of gloss. Marlow and Anderson (2013) have recently argued that the perception of gloss has three component dimensions. Two of these roughly correspond to the two specular components of the Ward reflectance model (see also Fleming et al., 2003; Pellacini, Ferwerda, & Greenberg, 2000). Specular contrast refers to the differences between the diffuse and specular components of reflection such that contrast is much higher for shiny black plastic than for shiny white plastic. Specular sharpness (or distinctness) refers to the steepness of the luminance gradients along the edges of highlights. This is typically controlled by varying roughness, but it can also be manipulated by blurring the pattern of illumination, or manipulating the curvature of surface bumps.

The third component of Marlow and Anderson's (2013) model is called coverage. It refers to the proportion of an object's surface that is covered by specular reflections. It is important to keep in mind that the highlights on shiny surfaces occur on regions where the surface normal bisects the angle between the

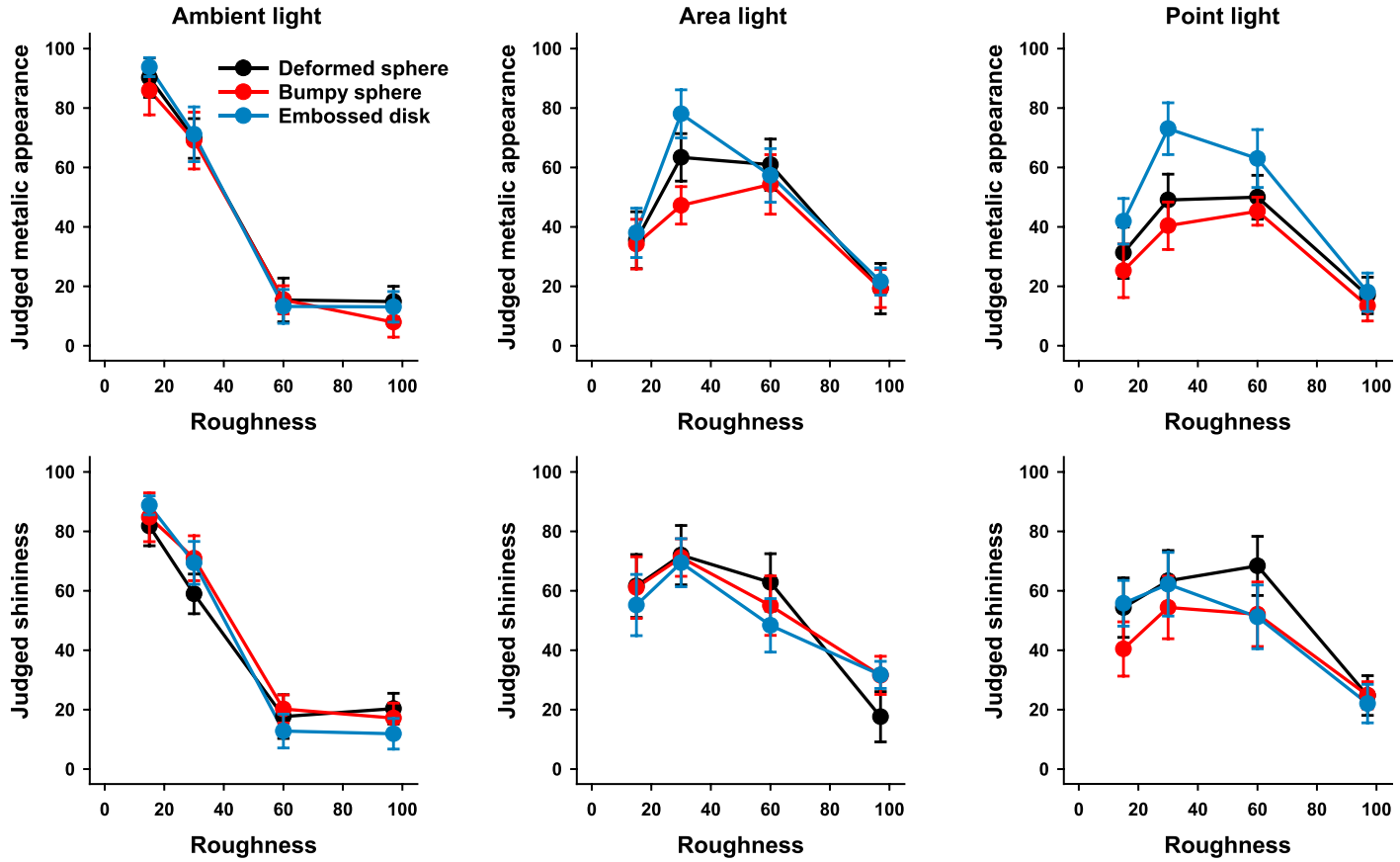

Figure 11. The judged metallic appearance (top) and shininess (bottom) for metal surfaces with four different levels of roughness. Error bars show the standard errors of the mean for each condition.

direction of illumination and the viewing direction. One way they manipulated coverage in their investigation was to increase the density of bumps on a surface, which increases the number of surface locations whose surface normals satisfy that criterion (see also Ho et al., 2008; Marlow et al., 2012). Another method employed by Marlow and Anderson to increase coverage was to adjust the direction of illumination for relatively flat surfaces so that highlights would spread over relatively large areas.

We believe it is the case that the spreading of highlights over large areas of a surface is what observers are referring to when they use the term *sheen*, and that this is an important source of information for the appearance of metal. Professional photographers use a couple of techniques to produce this effect (see Hunter et al., 2007). For relatively flat surfaces, sheen can be produced in the manner employed by Marlow and Anderson (2013) by positioning a light source at precisely the right location so that the surface normal bisects the viewing and illumination angles. A good example of this can be seen in the roughness 30 versions of the embossed disk in Figure 7. Note in particular how the highlights from the point and area lights spread across the entire flat region of the surface, which gives this object a more metallic appearance than the comparable conditions for the deformed or bumpy spheres. The ratings for those conditions shown in Figure 11 appear to confirm this observation, although there were no significant differences in observers' judgments for the three different objects in the overall pattern of results.

A more general technique for producing metallic sheen on most generic surfaces is to employ a pattern of illumination that has a smooth gradation of intensities over all directions, like the translucent white room used in the present experiment. Specular sheen can also be increased to some degree by increasing surface roughness, which blurs specular highlights and increases their spatial extent, although very high roughness values will eliminate highlights altogether.

Let us consider some specific examples. Note in Figures 6 through 8 how the low-roughness metal surfaces with ambient illumination are covered almost completely by specular reflections. This is in contrast to the low-roughness surfaces with isolated point or area lights, for which the highlights only occur in relatively small local regions and the surfaces are black everywhere else. These images are most commonly identified as black plastic. Interestingly, when the objects

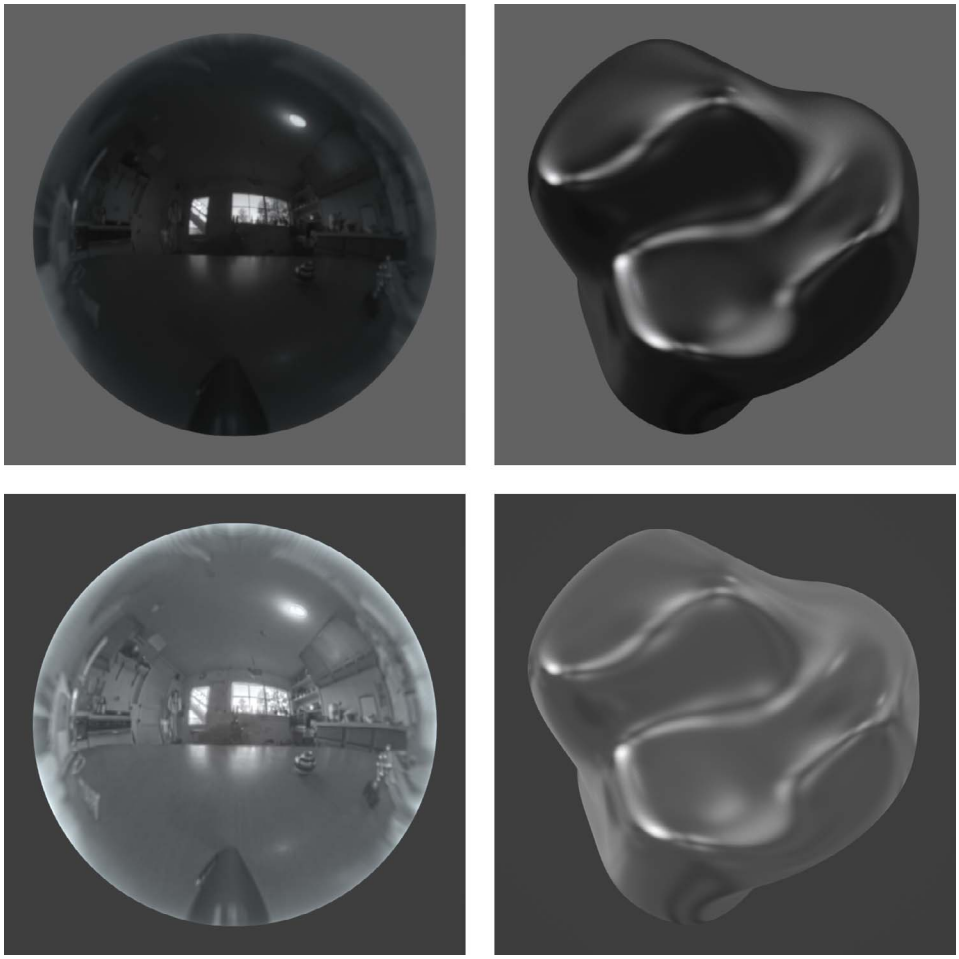

Figure 12. Images created using the kitchen light probe from the Debevec (1998) HDRI Gallery. The left column depicts a mirrored ball and the right column depicts a deformed chrome sphere with a roughness of 15. The exposures of these images have been adjusted so that they all have the same maximum luminance. The images in the top row show the entire dynamic range of the light map, whereas the ones in the bottom row were created using a tone-mapped version of the light map, in which the intensity of the direct light was dramatically reduced relative to the indirect ambient light. Note how the deformed sphere on the upper right appears as shiny black plastic, whereas as the one on the lower right appears as metal.

illuminated without ambient light are depicted with intermediate levels of roughness, the highlights spread over larger regions of the surface, and the ratings of metallic appearance are increased. It is important to keep in mind that for any given point on a purely specular surface, there is only a tiny range of incident directions for which any light will be reflected toward the point of observation. Thus, in order to produce a high proportion of specular coverage on a smoothly curved object, it is necessary to have sufficient ambient light in a scene so that each surface region is illuminated from a broad range of directions.

In order to reinforce this point, it is useful to consider the four images shown in Figure 12. All of these images were created using the *kitchen light probe* from the Debevec HDRI Gallery (Debevec, 1998). The image in the upper left panel shows the reflections of this illumination field on a perfectly smooth mirrored sphere. Note that the pattern of illumination has a very high dynamic range. Although there is some ambient light in the scene, it is dwarfed by the intensity of the direct light. If the camera exposure is adjusted to prevent saturation of the direct light, the effects of the ambient light have only a minimal influence on the resulting images. The upper right panel of Figure 12 shows the reflections of this illumination field on a deformed chrome sphere with a microscopic roughness of 15. Note, in that case, that much of the visible surface is black and that it appears as shiny black plastic. The scenes depicted in the bottom row of Figure 12 were illuminated using a transformed version of the kitchen light probe that was manually adjusted in Photoshop Creative Cloud (Adobe Systems, San Jose, CA) using the local adaptation tone mapping tool to reduce the intensity of the direct light relative to that of the indirect ambient light, while trying to maintain the

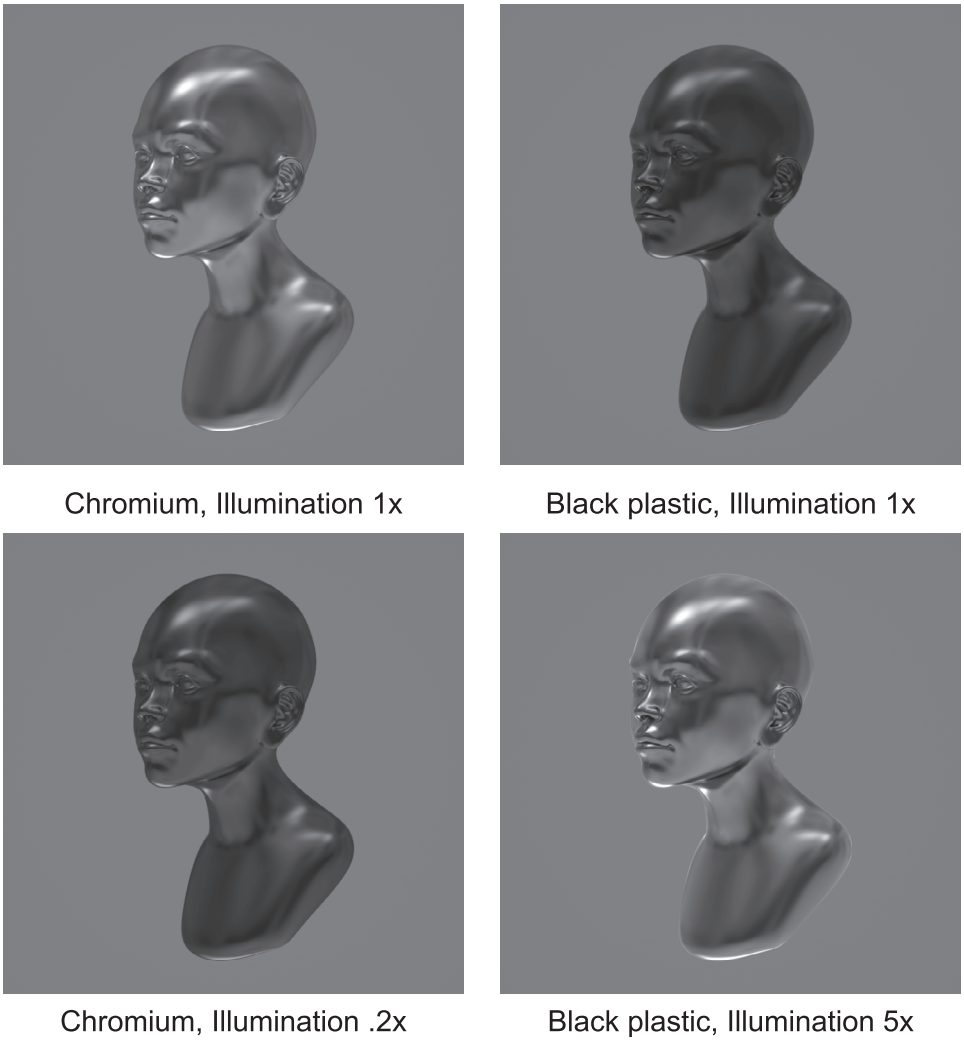

Figure 13. Images of a boy's bust illuminated by an HDRI light map of an atrium. The left column depicts a low roughness chrome material and the right column depicts a black plastic material with the specular properties of glass. The images in the top row have the same magnitude of illumination and camera exposure, and they are correctly identified as metal and black plastic, respectively. The metal material in the lower left panel has a reduced illumination and is identified incorrectly as black plastic, whereas the black plastic material in the lower right panel has an increased illumination and is incorrectly identified as metal.

high frequency details of the image. When this transformed light probe is used to illuminate the deformed chrome sphere in the lower right panel, the depicted material appears much more metallic. The tone mapping in this case structures the light in much the same way as the translucent white room used in the present experiment by softening the direct light and increasing the relative intensity of the indirect ambient light.

Based on these observations, we can now offer a tentative hypothesis about the perceptually defining characteristics of white plastic, black plastic and metal. White (or colored) plastic is perceived when diffuse and specular reflections are additively combined. Black plastic is perceived when there are no diffuse reflections, and specular highlights are confined to a relatively small proportion of the visible surface. Metal is perceived when there are no diffuse reflections, and specular reflections are spread out over most of the visible surface. The results of the present experiment and demonstrations suggest that these perceptual categories do not have sharp boundaries, and that they can be strongly influenced by the ambient light (or lack thereof) in a scene, and the microscopic roughness of a material.

Another important factor that can influence the perceptual distinction between metal and black plastic is the intensity of illumination (or camera exposure). As is shown in Figure 3, metals reflect a much higher proportion of the incident illumination than the specular reflections of nonmetal materials such as black plastic. Consider, for example, the two images of a

Figure 14. Images of a low roughness chrome bust illuminated by an HDRI light map of a banquet hall (see Figure 4). The one on the left appears as a shiny metal material. To create the image in the middle panel the light map was blurred, which produces the appearance of a shiny white material, and it was blurred even more for the image on the right, so that the depicted material appears matte.

boy's bust in the top row of Figure 13. Both images are illuminated by an HDRI light probe of an atrium, and they both have the same magnitude of illumination and the same camera exposure. The one on the left depicts a low roughness chrome material. It has a high coverage of specular reflections and is perceived as metal. The image on the right depicts a black plastic material. It has a relatively low coverage of specular reflections and is perceived as black plastic. However, it is important to keep in mind that variations in reflectance can be offset by variations in the magnitude of illumination or camera exposure. The bottom left panel of Figure 13 shows a low-roughness chrome material with reduced illumination that is perceived as black plastic, and the bottom right panel shows a black plastic material with increased illumination that is perceived as metal.

One last issue that is useful to consider concerns the perceptual distinction between metal materials with high specular coverage and matte, Lambertian reflections that can also cover the entire visible area of a surface. We suspect that this distinction may be based primarily on image contrast. Most illumination fields in the natural environment have substantial variations in intensity across different illuminant directions, which results in much higher contrast for purely specular surfaces than for purely matte surfaces. Figure 14 is designed to demonstrate what happens when these spatial variations in illuminant intensity are gradually eliminated. Each panel in this figure depicts a chrome bust of a young boy. The one in the left panel is illuminated using an HDRI light probe of a banquet hall (see Figure 4) with a spatial resolution of $6{,}250 \times 3{,}125$ pixels. Note how this produces a very compelling impression of a metallic surface. The object in the middle panel is illuminated by a distorted version of the same light probe that was blurred using a Gaussian kernel with a radius of 300 pixels. That object appears as a somewhat glossy white material. The light probe used in the right panel was blurred even more using a kernel radius of 600 pixels, so that the pattern of illumination is close to a Ganzfeld. Note in that case, that the object appears completely matte. This demonstration suggests that the appearance of metal may require a sufficient range of illuminant intensities in addition to a sufficient range of illuminant directions.

There have been several previous demonstrations in the literature to show that the appearance of surface materials can be significantly influenced by the pattern of illumination. Most of these have focused on the apparent glossiness of materials with a linear combination of diffuse and specular components (Doerschner et al., 2010; Fleming et al., 2003; Marlow & Anderson, 2012, 2013; Mooney & Anderson, 2014; Nishida & Shinya, 1998; Olkkonen & Brainard, 2010, 2011; Pont & te Pas, 2006; Zhang et al., 2015), although there are a couple of exceptions to this trend. For example, Fleming and Bülthoff (2005) have shown that the perception of translucency can be enhanced when objects are illuminated from behind, and Zhang et al. (2015) have reported that collimated light fields work best to bring out the apparent velvetiness of a surface. The present investigation has extended this general area of research to the perception of metal. Our empirical results show clearly that the presence of ambient illumination from a broad range of directions is a critical factor for surfaces to appear metallic, and the demonstration in Figure 14 suggests

that spatial variations in illuminant intensity may be another important requirement.

Acknowledgments

Commercial relationships: none.
Corresponding author: James T. Todd.
Email: todd.44@osu.edu.
Address: Department of Psychology, The Ohio State University, Columbus, OH, USA.

References

Anderson, B. L., & Kim, J. (2009). Image statistics do not explain the perception of gloss and lightness. *Journal of Vision*, *9*(11):10, 1–17, https://doi.org/10.1167/9.11.10. [PubMed] [Article]

Beck, J., & Prazdny, K. (1981). Highlights and the perception of glossiness. *Perception & Psychophysics*, *30*, 407–410.

Debevec, P. E. (1998). Rendering synthetic objects into real scenes: Bridging traditional and image-based graphics with global illumination and high dynamic range photography. In *SIGGRAPH 98, Proceedings of the 25th Annual Conference on Computer Graphics and Interactive Techniques*, Orlando, FL, July 19–24 (pp. 189–198).

Doerschner, K., Boyaci, H., & Maloney, L. T. (2010). Estimating the glossiness transfer function induced by illumination change and testing its transitivity. *Journal of Vision*, *10*(4):8, 1–9, https://doi.org/10.1167/10.4.8. [PubMed] [Article]

Doerschner, K., Fleming, R. W., Yilmaz, O., Schrater, P. R., Hartung, B., & Kertsen, D. (2011). Visual motion and the perception of surface material. *Current Biology*, *21*, 2010–2016.

Fleming, R. W., & Bülthoff, H. H. (2005). Low-level image cues in the perception of translucent materials. *ACM Transactions on Applied Perception*, *2*(3), 346–382.

Fleming, R. W., Dror, R. O., & Adelson, E. H. (2003). Real-world illumination and the perception of surface reflectance properties. *Journal of Vision*, *3*(5):3, 347–368, https://doi.org/10.1167/3.5.3. [PubMed] [Article]

Fleming, R. W., Wiebel, C., & Gegenfurtner, K. (2013). Perceptual qualities and material classes. *Journal of Vision*, *13*(8):9, https://doi.org/10.1167/13.8.9. [PubMed] [Article]

Ho, Y., Landy, M. S., & Maloney, L. T. (2008). Conjoint measurement of gloss and surface texture. *Psychological Science*, *19*, 196–204.

Hunter, F., Biver, S., & Fuqua, P. (2007). *Light, science & magic: An introduction to photometric lighting*. Amsterdam, the Netherlands: Elsevier.

Kim, J., Marlow, P. J., & Anderson, B. L. (2011). The perception of gloss depends on highlight congruence with surface shading. *Journal of Vision*, *11*(9):4, 1–19, https://doi.org/10.1167/11.9.4. [PubMed] [Article]

Kim, J., Marlow, P. J., & Anderson, B. L. (2012). The dark side of gloss. *Nature Neuroscience*, *15*(11), 1590–1595.

Koenderink, J. J. (1990) *Solid shape*. Cambridge, MA: MIT Press.

Marlow, P., & Anderson, B. L. (2013) Generative constraints on image cues for perceived gloss. *Journal of Vision*, *13*(14):2, 1–23, https://doi.org/10.1167/13.14.2. [PubMed] [Article]

Marlow, P. J., & Anderson, B. L. (2015). Material properties derived from three-dimensional shape representations. *Vision Research*, *115*, 199–208.

Marlow, P., Kim, J., & Anderson, B. L. (2011). The role of brightness and orientation congruence in the perception of surface gloss. *Journal of Vision*, *11*(9):16, 1–12, https://doi.org/10.1167/11.9.16. [PubMed] [Article]

Marlow, P., Kim, J., & Anderson, B. L. (2012). The perception and misperception of specular surface reflectance. *Current Biology*, *22*(20), 1909–1913.

Mingolla, E., & Todd, J. T. (1986). Perception of solid shape from shading. *Biological Cybernetics*, *53*, 137–151.

Mooney, S. W. J., & Anderson, B. L. (2014). Specular image structure modulates the perception of three-dimensional shape. *Current Biology*, *24*, 2737–2742.

Motoyoshi, I., & Matoba, H. (2012). Variability in constancy of the perceived surface reflectance across different illumination statistics. *Vision Research*, *53*, 30–39.

Motoyoshi, I., Nishida, S., Sharon, L., & Adelson, E. H. (2007). Image statistics and the perception of surface qualities. *Nature*, *447*, 206–209.

Nishida, S., & Shinya, M. (1998). Use of image-based information in judgments of surface-reflectance properties. *Journal of the Optical Society of America A*, *15*, 2951–2965.

Norman, J. F., & Todd, J. T. (1996). The discriminability of local surface structure. *Perception*, *25*, 381–398.

Olkkonen, M., & Brainard, D. H. (2010). Perceived

glossiness and lightness under real-world illumination. *Journal of Vision*, *10*(9):5, 1–19, https://doi.org/10.1167/10.9.5. [PubMed] [Article]

Olkkonen, M., & Brainard, D. H. (2011). Joint effects of illumination geometry and object shape in the perception of surface reflectance. *i-Perception*, *2*, 1014–1034.

Pellacini, F., Ferwerda, A. D., & Greenberg, P. (2000). Toward a psychophysically-based light reflection model for image synthesis. *ACM Transactions on Graphics*, *34*, 55–64.

Pont, S. C., & te Pas, S. F. (2006). Material illumination ambiguities and the perception of solid objects. *Perception*, *35*, 1331–1350.

Sharan, L., Rosenholtz, R., & Adelson, E. H. (2014). Accuracy and speed of material categorization in real-word images. *Journal of Vision*, *14*(9):12, 1–24, https://doi.org/10.1167/14.9.12. [PubMed] [Article]

Todd, J. T., & Mingolla, E. (1983). The perception of surface curvature and direction of illumination from patterns of shading. *Journal of Experimental Psychology: Human Perception and Performance*, *9*, 583–595.

Todd, J. T., & Norman, J. F. (1995). The visual discrimination of relative surface orientation. *Perception*, *24*, 855–866.

Todd, J. T., Norman, J. F., & Mingolla, E. (2004). Lightness constancy in the presence of specular highlights. *Psychological Science*, *15*, 33–39.

Vangorp, P., Barla, P., & Fleming, R. W. (2017). The perception of hazy gloss. *Journal of Vision*, *17*(5):19, 1–17, https://doi.org/10.1167/17.5.19. [PubMed] [Article]

Ward, G. J. (1994). The RADIANCE lighting simulation and rendering system. *Computer Graphics*, *28*(2), 459–472.

Wijntjes, M. W. A., Doerschner, K., Kucukoglu, G., & Pont, S. C. (2012). Relative flattening between velvet and matte 3D shapes: Evidence for similar shape-from-shading computations. *Journal of Vision*, *12*(1):2, 1–11, https://doi.org/10.1167/12.1.2. [PubMed] [Article]

Wijntjes, M. W., & Pont, S.C. (2010). Illusory gloss on Lambertian surfaces. *Journal of Vision*, *10*(9):13, 1–12, https://doi.org/10.1167/10.9.13. [PubMed] [Article]

Zhang, F., de Ridder, H., & Pont, S. C. (2015). The influence of lighting on visual perception of material qualities. In *Proceedings of SPIE 9394, Human Vision and Electronic Imaging XX*, 93940Q, https://doi.org/10.1117/12.2085021.